Published in final edited form as:
Acta Biomater. 2012 December ; 8(12): 4278–4284. doi:10.1016/j.actbio.2012.08.010.

Size-controlled Insulin Secreting Cell Clusters

Adam D. Mendelsohn[a], **Crystal Nyitray**[b], **Mark Sena**[a], and **Tejal A. Desai**[a,c,*]

Adam D. Mendelsohn: adam.mendelsohn@gmail.com; Crystal Nyitray: thecrystal.n@gmail.com; Mark Sena: msena505@gmail.com

[a]UC Berkeley – UCSF Graduate Program in Bioengineering, University of California at San Francisco and University of California at Berkeley, San Francisco, California, 94158

[b]Department of Chemistry and Chemical Biology, University of California at San Francisco, San Francisco, California, 94158

[c]Department of Bioengineering and Therapeutic Sciences, University of California at San Francisco, San Francisco, California, 94158

Abstract

An effective cure for type I diabetes from the transplantation of encapsulated pancreatic β-cell clusters has so far produced sub-optimal clinical outcomes. Previous efforts have not controlled the size of transplanted clusters, a parameter implicated in affecting long-term viability and the secretion of therapeutically sufficient insulin. Here we demonstrate a method based on covalent attachment of patterned laminin for fabricating uniformly size-controlled insulin-secreting cell clusters. We show that cluster size within the range 40-120 μm in diameter affects a variety of therapeutically relevant cellular responses including insulin expression, content, and secretion. Our studies elucidate two size-dependent phenomena: (1) as the cluster size increases from 40 μm to 60 μm, glucose stimulation results in a greater amount of insulin produced per cell; and (2) as the cluster size increases beyond 60 μm, sustained glucose stimulation results in a greater amount of insulin secreted per cell. Our study describes a method for producing uniformly sized insulin-secreting cell clusters, and since larger cluster sizes risk nutrient availability limitations, our data suggests that 100-120 μm clusters may provide optimal viability and efficacy for encapsulated β-cell transplants as a treatment for type I diabetes and that further *in vivo* evaluation is warranted.

[*]Corresponding author Tejal A. Desai, Professor, Dept. of Bioengineering and Therapeutic Sciences, UCSF MC 2520, Byers Hall Rm 203C, San Francisco, CA 94158-2330, Phone: office +1-415-514-4503, Fax: +1-415-514-4503, Tejal.desai@ucsf.edu.

AUTHOR CONTRIBUTIONS

ADM: Conception and design, collection and assembly of data, data analysis and interpretation, manuscript writing
CN: Collection and assembly of data, data analysis and interpretation, manuscript writing
MS: Collection and assembly of data, data analysis and interpretation
TAD: Conception and design, financial support, data analysis and interpretation, manuscript writing, final approval of manuscript

DISCLOSURE OF POTENTIAL CONFLICTS OF INTEREST

The authors declare no potential conflicts of interest.

Keywords

Transplantation; Islet; Patterning; Pancreatic β-cell; Insulinoma; Type I Diabetes; Microcontact Printing

1. INTRODUCTION

Development of a bioartificial pancreas began in 1933 when tissue containing insulin-secreting cells was first transplanted as a potential diabetes treatment.[1] Nearly eighty years later, human trials currently underway in New Zealand evaluating encapsulated islet transplants without immunosuppression report significant reductions in hypoglycemic events, but have yet to achieve reliable insulin independence. Transplantations of unencapsulated human cadaveric β-cell containing islets are currently available and provide at least one year of insulin independence for 80% of recipients.[2] While these pancreatic β-cells are able to sense glucose and secrete insulin at the appropriate level needed for glucose homeostasis, debilitating immunosuppression is required[3] and the availability of cadaveric islets is extremely limited.[4] Significant advances in encapsulation technologies over the past several decades promise to obviate the need for immunosuppression.[5, 6] Additionally, animal sources[7, 8] and human stem cell sources[9, 10] are being cultivated to overcome supply limitations. While these developments promise to overcome some of the limitations preventing wide-scale adoption of this therapeutic approach, efforts to control the size of transplanted clusters have been lacking.

Two independent size requirements must be satisfied in order to achieve viable islet transplants with sufficient insulin secretion. First, very small clusters do not exhibit therapeutically appropriate insulin secretion because of its dependence on sufficient cell-cell contact. For example, pancreatic β-cell pairs and monolayers secrete greater insulin per cell after glucose stimulation than isolated β-cells.[11, 12] Furthermore, glucose-dependent calcium oscillations, a characteristic of appropriately functioning islets, occur more frequently in cell clusters compared with isolated cells.[13] Second, excessively large clusters suffer from nutrient availability limitations. Relying solely on passive diffusion, oxygen and nutrient requirements are attained only when cells are within 100-200 μm from a capillary.[14-16] In fact, necrosis has been observed on the inside of large isolated islets.[17, 18] As expected from these results, islets smaller than 150 μm in size exhibit improved insulin secretion and viability in clinical studies than larger islets.[19] While cell encapsulation in a material with pore sizes small enough to inhibit the passage of antibodies protects transplants from the immune response,[20] the same material also inhibits the growth of new blood vessels and prevents access to perfusion that is essential for nutrient availability throughout large islets in the native pancreas.[21] Despite significant evidence supporting the impact that cluster-size may have on insulin secretion and viability of encapsulated transplants, to date there appears no study that either explicitly explores the insulin response to varying cluster-sizes or presents a method for fabricating uniformly sized clusters.

Here, we used the covalent microcontact printing of laminin, as described previously,[22] to fabricate size-controlled patterned insulin-secreting cell clusters. The rat insulinoma cell line

INS-1 (832/13) was selected for evaluation due to its dose-dependent glucose stimulated insulin secretion within physiologically relevant glucose conditions.[23, 24] We anticipate the use of stem cells to overcome supply limitations to clinical translation, as stem cells may be grown indefinitely prior to differentiation. Separately, we have demonstrated successful differentiation of size-controlled human embryonic stem cell clusters along the pancreatic lineage, as well as detachment of these clusters which may be necessary prior to transplantation.[25] Our data suggests the possibility of an optimal cluster size after evaluating its impact on insulin expression, content, and secretion from uniformly sized 40-120 μm insulin-secreting cell clusters. Successful production of size-controlled insulin-secreting clusters that appropriately balance the need for cell-cell contact and nutrient availability is a necessary step towards achieving long-term insulin independence for the millions that suffer from type I diabetes.

2. RESULTS

2.1. Consistent fabrication of uniformly-size insulin-secreting cell clusters

Insulin-secreting cells selectively adhered to patterned laminin resulting in uniformly size-controlled clusters on glass coverslips using a modified version of a previously described technique.[22] The extracellular matrix protein laminin was first microcontact printed from a lithographically-created polydimethylsiloxane stamp onto an aldehyde-functionalized glass coverslip. Subsequent incubation with a fluorescent protein enabled visualization of the areas surrounding the laminin pattern (Figure 1A). Laminin stamping was followed by the covalent attachment of polyethylene glycol, a polymer that resists cell attachment. Seeding density and incubation time were optimized to enable cells to neatly conform to varying laminin patterns (Figure 1B). Pattern uniformity across the entire coverslip was made possible for the first time by modifying the procedure for attaching polyethylene glycol from a one-step to a two-step reaction as visualized by 40 μm (Figure 1C), 60 μm (Figure 1D), and 120 μm (Figure 1E) circular cell patterns that are fixed and stained for nuclei and F-actin. We observed that the intensity of the nuclear stain correlates linearly with the number of nuclei within a given cluster (Supplementary Figure 1A). As expected, the distribution of the number of cells in a cluster is Gaussian, and the average number of cells in a cluster, measured over multiple coverslips, increases with the size of the laminin pattern (Supplementary Figure 1B and Supplementary Figure 1C).

2.2. Effect of Cluster Size on Insulin mRNA Expression and Secretion

After achieving confluency on patterned glass coverslips, insulin-secreting cells were pre-treated in low glucose to achieve basal insulin production which also reduced levels of insulin mRNA (Supplementary Figure 2) before exposure to high glucose. Insulin 2 mRNA expression, normalized to β-actin mRNA expression, was evaluated for 40 μm, 60 μm, and 120 μm clusters before, 15 minutes after, and 1 hour after high glucose stimulation. While no difference was observed prior to glucose stimulation, normalized insulin 2 mRNA expression was almost 2-fold smaller ($P<.021$) after 15 minutes of stimulation for the 40 μm clusters compared with the 60 μm and 120 μm clusters (Figure 2A). After 1 hour of stimulation, expression levels were the same for all measured cluster sizes.

Additionally, the effect of cluster size on insulin secretion was evaluated after GSIS. Samples were taken from wells containing patterned 40, 60, and 120 μm insulin-secreting cell clusters subjected to glucose starvation and then either continued glucose starvation or high glucose stimulation for 1 hour. Whereas insulin secretion from 40 μm clusters remained unchanged when incubated with high glucose, it was 2.5-fold and nearly 3.5-fold higher for 60 μm and 120 μm clusters, respectively (Figure 2B). Insulin secretion 15 minutes after stimulation was undetectable for all cluster sizes.

2.3. Effect of Cluster Size and Cell Number on Insulin and C-peptide Content

C-peptide content from patterned 832/13 insulinoma cells was evaluated as a surrogate for insulin content by first establishing colocalization of insulin and c-peptide immunofluorescence. Proinsulin is processed into insulin and c-peptide in an equimolar ratio; both products reside in the same secretory vesicles and are released simultaneously.[26, 27] Positive c-peptide staining is therefore used to verify the presence of de novo insulin synthesis as opposed to exogenously introduced insulin.[28] Immunofluorescence reveals colocalization of insulin (green) and c-peptide (red) (Supplementary Figure 3).

Since gap junction proteins modulate insulin secretion,[29] multiple cell layers, as opposed to monolayers, could positively impact the insulin response to glucose stimulation. Multilayer formation occurs when initially-formed clusters contain too many cells to fit in one layer on the printed laminin and pile up as they retreat from the cell-repulsive PEG.[22] While no c-peptide content differences were observed using quantitative imaging prior to glucose stimulation, c-peptide content in multilayered 60 μm clusters exceeded that of monolayered 60 μm clusters after 15 minutes of glucose stimulation (Figure 3a). Visualization of the c-peptide channel from representative images qualitatively confirms this effect, and zoomed-in section views of the cell clusters verifies the presence of a monolayer or multilayered cluster (Figure 4). This difference disappeared after stimulation was sustained for one hour (Figure 3a).

Additionally, normalized c-peptide staining intensity for 40, 60, 80, 100 and 120 μm circular monolayered cell clusters over the three glucose conditions under evaluation revealed the impact of size on the extent to which insulin is stored after production. 15 minutes after glucose stimulation, a 2-fold increase in insulin content over unstimulated clusters was seen for all but the 40 μm clusters (Figure 3b). This 2-fold change was not exceeded with increasing cluster size. Furthermore, 1 hour after glucose stimulation, smaller sized (40 μm and 60 μm) clusters contained greater c-peptide than larger sized (100 μm and 120 μm) clusters (Figure 3b). Representative images qualitatively confirm these effects (Figure 5). C-peptide localization analysis further reveals more uniformly distributed staining 15 minutes after stimulation, whereas the c-peptide in 40, 60, and 80 μm clusters appears localized to only a portion of the cells in each cluster.

3. DISCUSSION

This study suggests that as insulin-secreting cell cluster size increases from 40 μm to 120 μm, the insulin response to glucose stimulation is affected at two separate threshold sizes: the first results in greater insulin expression and translation shortly after glucose stimulation,

and the second results in more efficient insulin secretion after sustained glucose stimulation. After expression and subsequent translation, a number of post translational steps occur resulting in the storage of mature insulin and c-peptide awaiting secretion. [30] One previous simulation of β-cell behavior speculated that a minimum of 4 β-cell-β-cell contacts are required for insulin bursting coordination, and that this coordination improves upon addition of several more β-cells before reaching a plateau.[31] Characterization of our cell patterns revealed that 40 μm patterns contained on average between 6 and 7 cells per cluster, and 60 μm patterns contained on average between 15 and 16 cells per cluster (Supplementary Figure 1C). Our data supports this study's suggestion that insulin production behavior is affected by the number of β-cells in contact with each other, as well as the approximate number of cells required to effect such changes.

The existence of a second threshold cluster size enabling more efficient insulin secretion was less expected, and further exploration will be required prior to speculation of a responsible mechanism. Nonetheless, as the cluster size increased from 60 μm to 100 μm, c-peptide content after 1 hour of glucose stimulation decreased in a size-dependent fashion, with no additional decrease between 100 μm and 120 μm clusters. Instead of a concurrent reduction in insulin secretion over this time period, cells in 120 μm clusters on average responded with significantly greater insulin secretion (~3.5-fold) compared with cells in 60 μm clusters (~2.5-fold), although this result was not significant (Figure 2B). These two observations, when taken together, suggest that the larger cluster sizes secrete insulin more quickly, with less storage, after sustained glucose stimulation.

We realize that evaluation of insulin secretion included a portion of clusters with more cells than those used in content analyses, some of which were multilayered in nature (Supplementary Figure 1B). We have also demonstrated that multilayered 60 μm clusters contain more c-peptide 15 minutes after glucose stimulation than monolayered 60 μm clusters (Figure 3). However, multilayered clusters did not contain reduced c-peptide compared with monolayered clusters after 1 hour of sustained glucose stimulation (Figure 4), supporting the proposal that a second size-dependent threshold enabling more efficient insulin secretion exists, and that multilayered 60 μm clusters do not exceed this threshold. After considering all of these factors, our data suggests that 120 μm cell clusters secrete insulin more rapidly during sustained exposure to glucose after expression and translation than 60 μm cell clusters. Furthermore, since 100 μm clusters exhibited similarly low c-peptide content after sustained glucose simulation, the threshold size for achieving more rapid insulin secretion is likely between 80 and 100 μm.

The oxygen levels associated with the *in vivo* environment surrounding a transplant will be significantly less than the incubator oxygen levels under which the experiments reported here were performed. The superiority of islets smaller than 150 μm in a human study provides some confidence that the 100-120 μm cluster size recommended by this *in vitro* study may be sufficiently small to achieve sufficient *in vivo* nutrient availability[19]. However, any encapsulation material that prevents the need for immunosuppression will contribute to nutrient availability limitations, the effects of which will need to considered in the design of the encapsulation material and evaluated *in vivo* before an optimal cluster size within a given encapsulation material can be definitively identified.

Multiple methods exist that would enable subsequent transplantation of these patterned clusters. First, the clusters could be transplanted in a patterned sheet, similar to a concept described previously and still in development. [32] This approach would require cell patterning to occur on a biocompatible substrate, or the transfer of patterned clusters to a biocompatible material. Second, microcapsules can encapsulate size-controlled clusters that are dislodged either naturally over time[25] or with exposure to collagenase-dispase (Supplementary Figure 5). Both of these approaches will require further optimization for parameters affecting nutrient availability that have been extensively reviewed elsewhere.[6] Alternatively, immunosuppressed transplantation of size-controlled clusters via the portal vein may improve clinical outcomes without requiring cluster organization optimization. The insulinoma cells used in this study are not ideal candidates for transplantation, in part due to the immortalized nature of the cell line. We considered the use of primary β-cells from MIP-GFP mice, but the number of cells necessary for these studies would require the use of hundreds of animals. Instead, we are separately investigating the differentiation of human embryonic stem cells, which can be proliferated indefinitely prior to differentiation, into 120 μm size-controlled clusters along the pancreatic lineage, which become 100 μm spherical clusters when released.[25] Regardless of the encapsulation approach, incorporation of size-controlled clusters into encapsulated transplantation therapy promises to overcome one of the few remaining challenges impeding this therapy from achieving successful outcomes.

4. EXPERIMENTAL SECTION

4.1. Preparation of laminin patterns on aldehyde-terminated glass cover slips

Clean dry plasma-treated glass cover slips were aldehyde-functionalized according to a procedure previously described[22], with a modification that prior to and after glutaraldehyde incubation sonicating with a 70:30 ethanol:Milli-Q water mixture instead of only Milli-Q, which improved patterned consistency compared with the previous method. We speculate that the improved patterning was the result of better removal of loosely attached glutaraldehyde. Laminin was covalently attached through microcontact printing from polydimethylsiloxane (PDMS) stamps using previously described techniques[22], with design modifications to the lithography mask to create 40-120 μm circular patterns evaluated in this study. The images of fluorescein isothiocyanate-conjugated bovine serum albumin (FITC-BSA) surrounding laminin patterns were taken with a wide-field fluorescent microscope (Olympus BX60).

4.2. Covalent attachment of PEG

After PDMS stamping of laminin on aldehyde-terminated glass cover slips, the coverslips were incubated with 25 μL of 3 mM methoxypolyethylene glycol-amine in methanol for >12 hours to quench unreacted aldehyde groups, followed by reduction in sodium cyanoborohydride in methanol (>8 mM).

4.3. Cell Culturing and Glucose Stimulated Insulin Secretion (GSIS)

INS-1 (832/13) cells were cultured using previously described methods[22] on patterned coverslips in 12-well plates. Cells were seeded in the same media, except RPMI 1640 w/

HEPES (Invitrogen) was replaced with RPMI 1640 w/o glucose (Invitrogen) and HEPES (Cell Culture Facility, San Francisco) and glucose (Cell Culture Facility, San Francisco) were added separately, at 8.33×10^4 cells/cm^2 on 40 μm patterned coverslips, 2.5×10^5 cells/cm^2 on 60 μm patterned coverslips, and 5×10^5 cells/cm^2 on 120 μm patterned coverslips. After 18-20 hours, pattern confluency was achieved and the cells were rinsed with 1 mL of a HEPES balanced salt solution described elsewhere[23], and then incubated in 1 mL of the same solution for 2 hours.

4.4. Insulin mRNA Expression

Insulin messenger ribonucleic acid (mRNA) expression was evaluated using an Applied Biosystems StepOnePlus Real-Time Polymerase Chain Reaction (PCR) System. Cells were lysed with TRIzol (Invitrogen) and total RNA was extracted with chloroform (Sigma A.C.S. grade >99.8%). cDNA was synthesize with iScript cDNA Synthesis Kit (Biorad). Reverse transcriptase-PCR (RT-PCR) was performed using SYBR green FAST mix (Applied Biosystems). The expression level of insulin 2 was normalized against β-actin using a standard curve method (See Table 1 for primers), and the results were analyzed with the Version 2.0 software.

4.5. Insulin Secretion

Insulin secretion was evaluated using an ultrasensitive rat insulin enzyme-linked immunosorbent assay (ELISA) kit (Mercodia). 40 μm, 60 μm, and 120 μm patterned coverslips, after 2 hours in the above glucose-free solution, were then either exposed to 1 mL of the same glucose-free solution or 1 mL of a 15 mM glucose created by adding the appropriate amount of D-glucose to the glucose-free solution at 37°C. After 1 hour, samples from each well were spun at 1500 × g, supernatants removed, and the concentrations of insulin, correlated to a standard curve using human insulin (Sigma), were determined by measuring the absorbance at 450 nm at the completion of the ELISA.

4.6. Characterization of Cell Patterning

Coverslips with patterned confluent clusters were rinsed with phosphate-buffered saline (PBS), fixed in 3.7% formaldehyde in PBS solution for 15 minutes, permeabilized with 0.5% Triton X-100 solution for 15 minutes, exposed to Alexa Fluor 488 Phalloidin (165 nM in PBS) to stain the F-actin, and DAPI (4’,6-diamidino-2-phenylindole, 300 nM in PBS) to stain the nuclei. Coverslips were imaged using wide-field fluorescent microscopy (Nikon Eclipse Ti-E motorized inverted microscope) with a 4x objective, and an 8×8 large image was obtained using NIS-elements 3.1 to visualize the entire patterned area. Image analysis was performed with NIS-elements 3.1.

4.7. Evaluation of c-peptide content

832/13 insulinoma cells were seeded using the same 5 mM glucose media described above onto patterned coverslips with a combination of 40 μm, 60 μm, 80 μm, 100 μm, and 120 μm circular laminin patterns at 2×10^5 cells/cm^2, or on 60 μm circular laminin patterns at 4×10^5 cells/cm^2. 18-20 hours later, pattern confluency was achieved on the combined patterned coverslips, and both confluent monolayers as well as multilayered clusters were present on

the 60 μm patterned coverslips. Coverslips were then rinsed with 1 mL of a HEPES balanced salt solution described elsewhere[23] with 0.2% essentially fatty acid free bovine serum albumin (BSA) and 0 mM glucose, and subsequently exposed to incubation in 1 mL of the same solution for 2 hours. Immediately prior to, 15 minutes after, and 1 hour after subsequent exposure to a 15 mM glucose solution, the cells were fixed with a solution of 3.7% formaldehyde in PBS solution for 15 minutes, permeabilized with 0.5% Triton X-100 solution for 15 minutes, immunostained with 1 μg/mL of rabbit anti-c-peptide (Cell Signaling) and/or 2 μg/mL mouse monoclonal anti-insulin (Santa Cruz Biotech) overnight at 4°C with 5% goat serum in buffer (13 mM dipotassium phosphate, 150 mM sodium chloride and 0.2% Tween 20, pH 7.5; same buffer used as follows unless otherwise specified). The coverslips were then rinsed thoroughly with buffer prior to incubation with 10 μg/mL donkey anti-mouse IgG Alexa Fluor 488 (Invitrogen) and/or goat anti-rabbit IgG Alexa Fluor 633 (Invitrogen) for 1 hour at room temperature. The cells were rinsed with buffer thoroughly before staining the actin cytoskeleton with 165 nM Alexa Flour 568 Phalloidin in PBS (Invitrogen) for 30 minutes. The nuclei were stained by sandwiching 3 μL of SlowFade Gold antifade reagent with DAPI (Invitrogen) between a microscope slide and a patterned coverslip, followed by nail polish to adhere the coverslip to the microscope slide.

Spinning disk confocal microscopy (Nikon Eclipse Ti-E motorized inverted microscope with Yokogawa CS22 Spinning Disk Confocal from Solamere Technology Group, Acquisition with Micro-Manager) was used to visualize the clusters. The cell borders of 0.25 μm-thick z-stacks were defined by the phalloidin and image intensity data within the confines of this volume was used for analysis using NIS-Elements. Lack of significant photobleaching was confirmed by evaluating five subsequent identical images for intensity differences at the laser power settings used.

5. CONCLUSIONS

In conclusion, we describe a method for fabricating uniformly size-controlled insulin-secreting cell clusters through covalent microcontact printing of laminin on aldehyde-functionalized coverslips. We demonstrate that cluster-size affects the insulin response to glucose stimulation in a therapeutically relevant manner. Finally, the results of our studies suggest that, among the sizes evaluated here, 100-120 μm clusters demonstrate the greatest promise for encapsulated transplantation therapy for treating type I diabetes.

Supplementary Material

Refer to Web version on PubMed Central for supplementary material.

Acknowledgments

This work was supported by the Juvenile Diabetes Research Foundation (JDRF grant awards 1-2010-152), the Sandler Family Foundation and NIH Training Grant T32 DK07418. Images were taken at the Nikon Center at UCSF with the assistance of Kurt Thorn, Sebastien Peck, and Alice Thwin. The authors would also like to thank Dr. Christopher Newgard for providing the 832/13 insulinoma cell line.

References

1. Bisceglie V. Uber die antineoplastiche Immunitat. E Krebsforsch. 1933; 40:141–158.
2. Shapiro AM, Ricordi C, Hering B. Edmonton's islet success has indeed been replicated elsewhere. Lancet. 2003; 362(9391):1242. [PubMed: 14568760]
3. Penn I. Post-transplant malignancy: the role of immunosuppression. Drug Saf. 2000; 23(2):101–13. [PubMed: 10945373]
4. Matsumoto S, et al. Estimation of donor usability for islet isolation with the modified Ricordi method. Transplant Proc. 2008; 40(2):362–3. [PubMed: 18374068]
5. Mendelsohn A, Desai T. Inorganic nanoporous membranes for immunoisolated cell-based drug delivery. Adv Exp Med Biol. 2010; 670:104–25. [PubMed: 20384222]
6. Wilson JT, Chaikof EL. Challenges and emerging technologies in the immunoisolation of cells and tissues. Adv Drug Deliv Rev. 2008; 60(2):124–45. [PubMed: 18022728]
7. Elliott RB, et al. Live encapsulated porcine islets from a type 1 diabetic patient 9.5 yr after xenotransplantation. Xenotransplantation. 2007; 14(2):157–61. [PubMed: 17381690]
8. Thanos CG, Elliott RB. Encapsulated porcine islet transplantation: an evolving therapy for the treatment of type I diabetes. Expert Opin Biol Ther. 2009; 9(1):29–44. [PubMed: 19063691]
9. Kroon E, et al. Pancreatic endoderm derived from human embryonic stem cells generates glucose-responsive insulin-secreting cells in vivo. Nat Biotechnol. 2008; 26(4):443–52. [PubMed: 18288110]
10. Van Hoof D, D'Amour KA, German MS. Derivation of insulin-producing cells from human embryonic stem cells. Stem Cell Res. 2009; 3(2-3):73–87. [PubMed: 19766074]
11. Meda P, et al. Rapid and reversible secretion changes during uncoupling of rat insulin-producing cells. J Clin Invest. 1990; 86(3):759–68. [PubMed: 1697604]
12. Brereton HC, et al. Homotypic cell contact enhances insulin but not glucagon secretion. Biochem Biophys Res Commun. 2006; 344(3):995–1000. [PubMed: 16643853]
13. Jonkers FC, et al. Influence of cell number on the characteristics and synchrony of Ca2+ oscillations in clusters of mouse pancreatic islet cells. J Physiol. 1999; 520(Pt 3):839–49. [PubMed: 10545148]
14. Orive G, et al. Biocompatibility of alginate-poly-L-lysine microcapsules for cell therapy. Biomaterials. 2006; 27(20):3691–700. [PubMed: 16574222]
15. Martin Y, Vermette P. Bioreactors for tissue mass culture: design, characterization, and recent advances. Biomaterials. 2005; 26(35):7481–503. [PubMed: 16023202]
16. Muschler GF, Nakamoto C, Griffith LG. Engineering principles of clinical cell-based tissue engineering. J Bone Joint Surg Am. 2004; 86-A(7):1541–58. [PubMed: 15252108]
17. De Vos P, et al. Why do microencapsulated islet grafts fail in the absence of fibrotic overgrowth? Diabetes. 1999; 48(7):1381–8. [PubMed: 10389842]
18. O'Sullivan ES, et al. Rat islet cell aggregates are superior to islets for transplantation in microcapsules. Diabetologia. 2010; 53(5):937–45. [PubMed: 20101386]
19. Lehmann R, et al. Superiority of small islets in human islet transplantation. Diabetes. 2007; 56(3): 594–603. [PubMed: 17327426]
20. Desai TA, et al. Microfabricated biocapsules provide short-term immunoisolation of insulinoma xenografts. Biomed Microdevices. 1999; 1(2):131–8. [PubMed: 16281113]
21. Ballian N, Brunicardi FC. Islet vasculature as a regulator of endocrine pancreas function. World J Surg. 2007; 31(4):705–14. [PubMed: 17347899]
22. Mendelsohn AD, et al. Patterning of mono- and multilayered pancreatic beta-cell clusters. Langmuir. 2010; 26(12):9943–9. [PubMed: 20218546]
23. Hohmeier HE, et al. Isolation of INS-1-derived cell lines with robust ATP-sensitive K+ channel-dependent and -independent glucose-stimulated insulin secretion. Diabetes. 2000; 49(3):424–30. [PubMed: 10868964]
24. Kuehn C, et al. Culturing INS-1 cells on CDPGYIGSR-, RGD- and fibronectin surfaces improves insulin secretion and cell proliferation. Acta Biomater. 2012; 8(2):619–26. [PubMed: 22085924]

25. Van Hoof D, et al. Differentiation of human embryonic stem cells into pancreatic endoderm in patterned size-controlled clusters. Stem Cell Res. 2011 In Press.

26. Block MB, et al. Sequential changes in beta-cell function in insulin-treated diabetic patients assessed by C-peptide immunoreactivity. N Engl J Med. 1973; 288(22):1144–8. [PubMed: 4633551]

27. Steiner DF, et al. Insulin biosynthesis: evidence for a precursor. Science. 1967; 157(789):697–700. [PubMed: 4291105]

28. Rajagopal J, et al. Insulin staining of ES cell progeny from insulin uptake. Science. 2003; 299(5605):363. [PubMed: 12532008]

29. Meda P. Cx36 involvement in insulin secretion: characteristics and mechanism. Cell Commun Adhes. 2003; 10(4-6):431–5. [PubMed: 14681053]

30. Gold G, et al. Heterogeneity and compartmental properties of insulin storage and secretion in rat islets. J Clin Invest. 1982; 69(3):554–63. [PubMed: 7037852]

31. Nittala A, Ghosh S, Wang X. Investigating the role of islet cytoarchitecture in its oscillation using a new beta-cell cluster model. PLoS One. 2007; 2(10):e983. [PubMed: 17912360]

32. Storrs R, et al. Preclinical development of the Islet Sheet. Ann N Y Acad Sci. 2001; 944:252–66. [PubMed: 11797674]

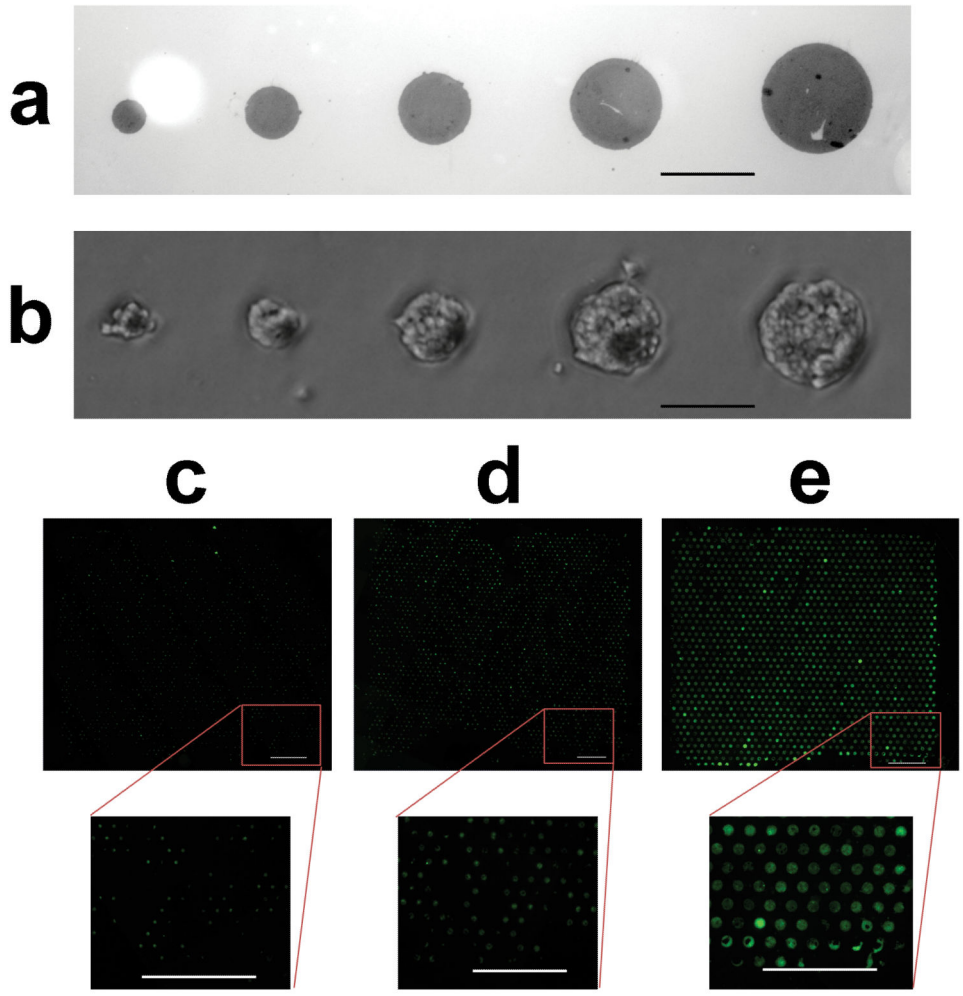

Figure 1. Cells seeded on patterned laminin become uniform size-controlled clusters

(a) 40, 60, 80, 100 and 120 μm laminin-patterned glass coverslips were visualized after incubation with fluorescein isothiocyanate-conjuated bovine serum albumin (FITC-BSA) before polyethylene glycol (PEG) deposition, scale bar – 100 μm. (b) Bright-field microscopy verified conformation of 832/13 rat insulinoma cells to patterned laminin after PEG deposition, scale bar – 100 μm. Fluorescent staining of nuclei (DAPI, blue) and F-actin (Alexa Fluor 488 Phalloidin, green) illustrates the uniformity of (c) 40 μm, (d) 60 μm, and (e) 120 μm patterns after seeded cells achieved confluency, scale bars = 1 mm.

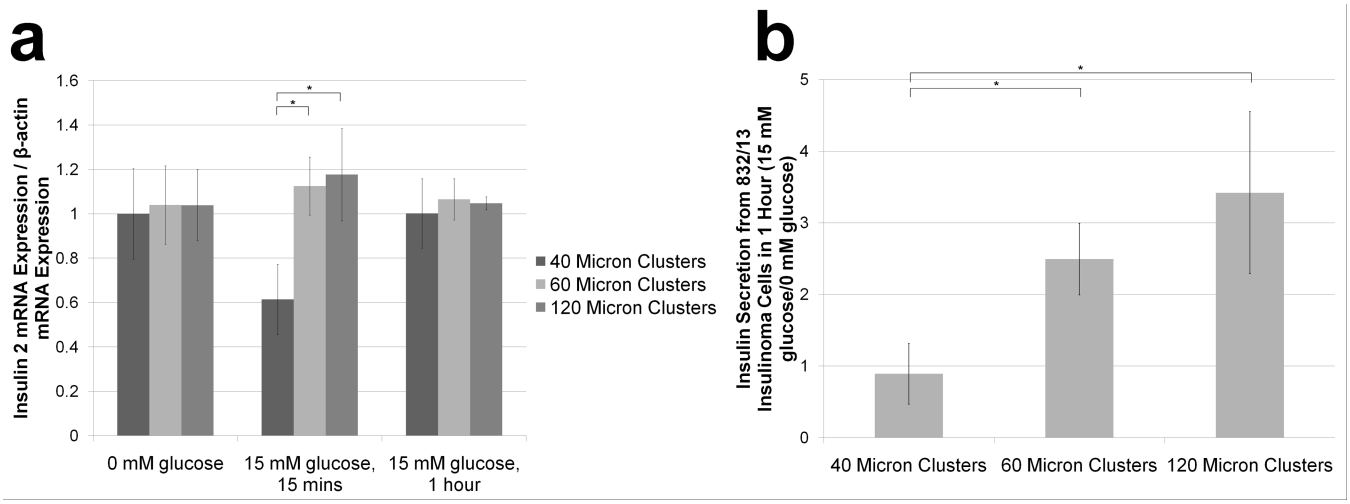

Figure 2. Normalized insulin 2 mRNA expression and normalized insulin secretion increases with larger cluster sizes

(a) RT-PCR was used to determined normalized insulin 2 mRNA expression for 40, 60, and 120 μm patterned confluent clusters 15 minutes after and 1 hour after 832/13 insulinoma cells were exposed to GSIS (data normalized to the average of the 40 μm clusters for each glucose condition). Additionally, (b) the impact of glucose stimulation on insulin secretion from 40 μm, 60 μm, and 120 μm clusters was determined by normalizing measured insulin secretion over 1 hour from clusters stimulated with 15 mM glucose (n=3) to clusters stimulated with 0 mM glucose that mimics basal secretion levels (n=3) for each cluster size. Data is presented as an average ± standard deviation. Statistical significance for the comparison of multiple groups was confirmed for each group indicated with an * using a Holm-Sidak test with α=.05 after performing an analysis of variances (ANOVA).

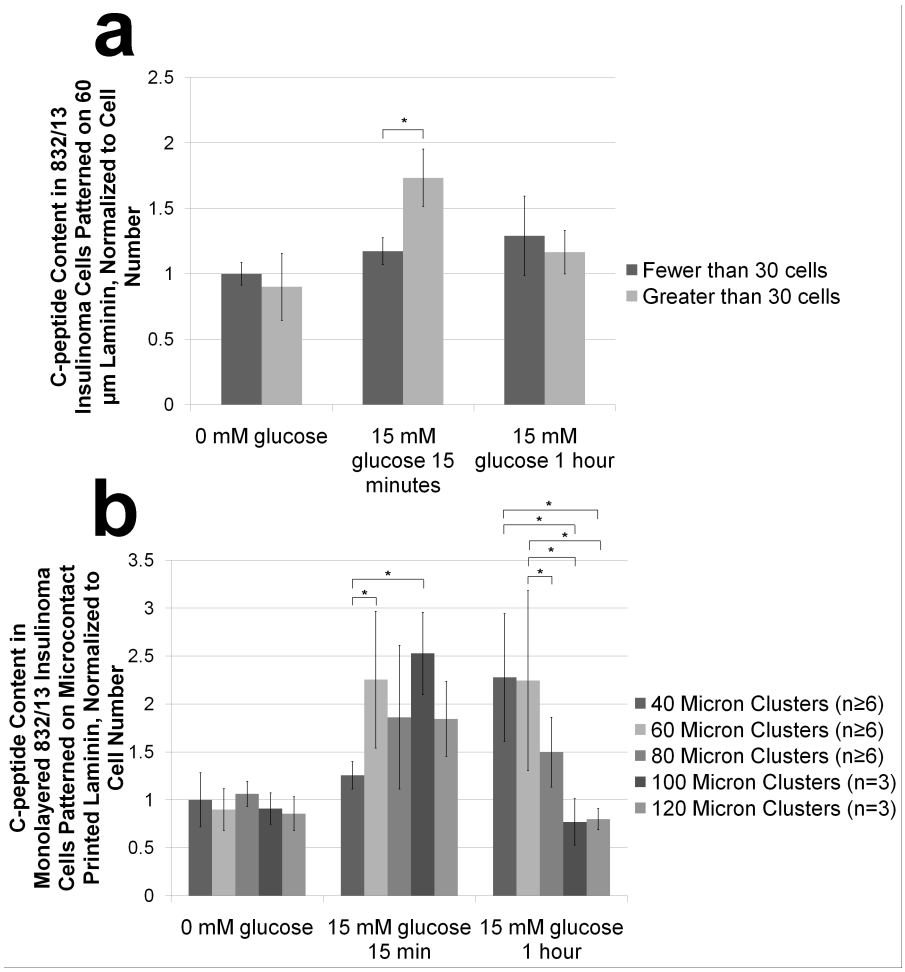

Figure 3. Semi-quantitative immunocytochemistry reveals effects of cluster size on normalized c-peptide content under different glucose conditions

832/13 insulinoma cell clusters are fixed, permeabilized and stained for c-peptide, F-actin and nuclei before, 15 minutes after, and 1 hour after glucose stimulation. Confocal images are acquired and total intensity of c-peptide staining is normalized to the nuclear stain intensity which correlates linearly with the number of nuclei (Supplementary Figure 4). (a) Quantified normalized c-peptide intensity was then determined between monolayered and multilayered clusters for each glucose condition (data is normalized to the average of monolayered clusters before glucose stimulation). (b) Normalized c-peptide intensity is also evaluated between monolayered clusters on a single coverslip containing 40, 60, 80, 100 and 120 µm are compared to each other for each glucose condition (data is normalized to the average of the 40 µm clusters before glucose stimulation). Data is presented as an average ± standard deviation. Statistical significance is indicated with an * and was established using the Student-Newman-Keuls Test with a α=.05 after performing an ANOVA.

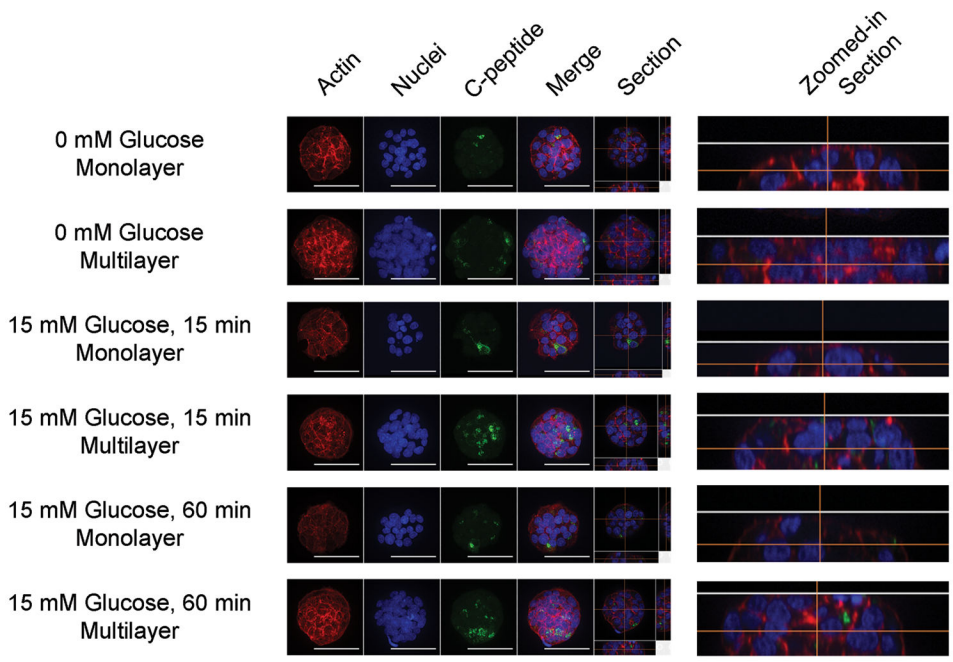

Figure 4. Confocal imaging reveals effect of multiple cell layers on c-peptide content under different glucose conditions

832/13 insulinoma cells were grown to confluency on glass coverslips that only have 60 μm patterns. Cell clusters were fixed, permeabilized, and stained for F-actin, nuclei, and c-peptide. Representative confocal sectioned z-stacked images revealed both monolayered (<30 cells) and multilayered (>30 cells) clusters. A maximum intensity projection enabled visualization of staining throughout the z-stacks (actin, nuclei, c-pep, and merge). One representative slice of the z-stack is displayed to the right of the maximum intensity projections (section), and the zoomed in section view verifies that the cell clusters are either in a monolayer or in multiple layers. Scale bar = 50 μm.

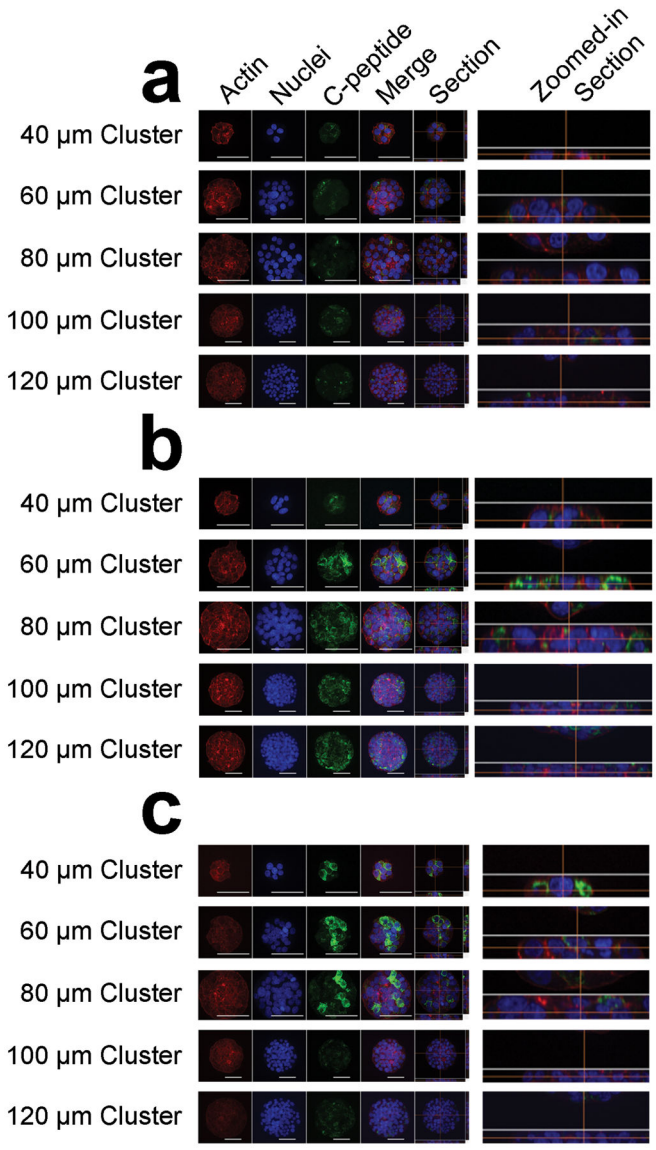

Figure 5. Confocal imaging reveals effect of monolayered cluster size on c-peptide content under different glucose conditions

832/13 insulinoma cells were grown to confluency on glass coverslips that have a combination of 40, 60, 80, 100 and 120 μm patterns. Cell clusters were fixed (a) just prior, (b) 15 minutes after, and (c) 1 hour after glucose stimulation, permeabilized, and stained for F-actin, nuclei, and c-peptide. Confocal z-stack images are taken throughout each cluster. A maximum intensity projection enabled visualization of staining throughout the z-stacks (actin, nuclei, c-pep, and merge). One representative slice of the z-stack is displayed to the right of the maximum intensity projections (section), and the zoomed in section view verifies that the cell clusters are in a monolayer. Scale bar = 50 μm.

Table 1

RT-PCR Primers.

INSULIN 2	Forward: 5'-GAA GTG GAG GAC CCA CAA GT-3' Reverse: 5'-AGT GCC AAG GTC TGA AGG TC-3'
β-ACTIN	Forward: 5'-CAA CCG TGA AAA GAT GAC CCA GA-3' Reverse: 5'-ACG ACC AGA GGC ATA CAG GGA C-3'